IEEE Access
Multidisciplinary : Rapid Review : Open Access Journal

Received July 26, 2021, accepted August 13, 2021, date of publication August 20, 2021, date of current version August 30, 2021.
Digital Object Identifier 10.1109/ACCESS.2021.3106327

Tactile Servoing Based Pressure Distribution Control of a Manipulator Using a Convolutional Neural Network

CHEN-TING WEN[1], SHOGO ARAI[1], (Member, IEEE), JUN KINUGAWA[2], (Member, IEEE), AND KAZUHIRO KOSUGE[3,4]
[1]Department of Robotics, Graduate School of Engineering, Tohoku University, Sendai 980-8579, Japan
[2]Physics and System Engineering Course, Faculty of Symbiotic Systems Science, Fukushima University, Fukushima 960-1296, Japan
[3]Center for Transformative AI and Robotics, Graduate School of Engineering, Tohoku University, Sendai 980-8579, Japan
[4]Department of Electrical and Electronic Engineering, Faculty of Engineering, The University of Hong Kong, Hong Kong
Corresponding author: Chen-Ting Wen (wen.chen.ting.r4@dc.tohoku.ac.jp)

ABSTRACT In this paper, we propose a novel tactile servoing based pressure distribution control scheme of a manipulator using a convolutional neural network (CNN). The CNN significantly improves the performance of the tactile servoing scheme compared to the one based on the tactile Jacobian. LeNet-5, originally proposed for image classification problems, is applied to represent a nonlinear relationship between current and desired pressure distributions and the robot velocity command by using mean squared error as the loss function. In the proposed control scheme, the trained CNN directly generates the velocity command of the manipulator so that the pressure distribution converges to a given desired pressure distribution. Validation experiments are carried out to evaluate the performance of the proposed control scheme. Experimental results show that the proposed tactile servoing control scheme has better performance than the Jacobian-based tactile servoing control scheme.

INDEX TERMS Manipulator control, pressure distribution control, tactile servoing, convolutional neural network.

I. INTRODUCTION

The sense of touch is one of the most important basic sensory functions of human beings, alongside the sense of sight, hearing, taste, and smell. The sense of touch is provided on the entire surface of the human body, and it plays a particularly important role in physical interactions with the environment when using hands. Humans routinely perform several tasks using their entire hands or palms based on tactile sensation feedback, such as applying cosmetics and massaging stiff shoulders. The tactile sensation is indispensable for physical interaction with the environment.

Robots with tactile sensation have been proposed to realize human-like skillful manipulation and physical interaction with the environment. In [1], Mukai *et al.* proposed a robot system, RIBA, for lifting and transferring a patient from a bed to a wheelchair with dual robot arms. RIBA is equipped with smart rubber sensors for detecting the pressure distribution of its arms. The smart rubber sensor was used for both, the tactile guidance of the robot and monitoring the pressure distribution between the robot arms and the patient. The pressure distribution itself was not controlled in this system.

Khoramshahi *et al.* have proposed a unified motion-force control approach for physical human-robot interaction and developed a robot for massage therapy on the forearm [2]. Luo *et al.* have proposed a robotic tapping massage using an impedance control scheme to ensure a safe tapping motion [3]. Wang and Whitney have proposed a robot, which can shave a human's beard via teleoperation [4]. The robot, equipped with fluid-based soft actuators, can safely shave a human's beard by using the feedback of the internal fluid pressure of the actuators. Compliant motion control schemes were implemented for physical human-robot interaction in these systems.

Real-time control of a robot motion via tactile feedback was proposed by Berger and Khosla [5]. In the proposed system, the manipulator was controlled so as to track the edges of an object in real-time by using the Hough Transform of the threshold tactile image [5]. The use of image-based visual servoing for control of dexterous hands using finger-tip tactile

The associate editor coordinating the review of this manuscript and approving it for publication was Saeid Nahavandi.

arrays was suggested by Weiss *et al.* [6]. Inspired by that paper, P. Sikka and H. Zhang *et al.* proposed a control scheme using features derived from tactile images and applied it to the rolling task of a cylindrical pin on a planar surface [7].

N. Chen and H. Zhang *et al.* further extended the approach in [7] to a more general scheme of a tactile servo for performing point and edge contacts with curved and planar sensing surfaces [8]–[11]. Li *et al.* proposed a control framework using task-dependent projector matrices for a whole set of tactile servoing tasks with task specific tactile interaction patterns [12]. Kappassov *et al.* proposed an external hybrid tactile position controller to realize more general tasks [13]. All of these tactile servo schemes were designed using the geometric tactile features derived from tactile image moments [8]–[11], principle component analysis of the tactile image [12], among others [13]. The selection and design of an appropriate feature for each task are required for the tactile servoing based on the geometric tactile features.

In order to avoid this problem, Wen *et al.* proposed to employ raw pressure distribution data as the tactile feature [14]. The control input is computed using the deviation between current and desired pressure distributions, and the tactile Jacobian [14]. The tactile servoing control scheme using tactile Jacobian works well when an initial contact state is close to the desired one, since the linearity assumption for the use of the tactile Jacobian holds only in the vicinity of the desired pressure distribution.

This paper proposes a novel tactile servoing control scheme using a convolutional neural network (CNN) to represents the nonlinear relationship [15] between current and desired pressure distributions and robot motion. In the proposed control scheme, the desired velocity of the end-effector is predicted directly from the measured and desired pressure distributions using the CNN. We organize this paper as follows. Section II describes an overview of the tactile servoing control scheme using constant tactile Jacobian. Section III introduces the neural network used in the tactile control scheme. Section IV introduces the experimental results that compare the performance of the proposed method to the constant tactile Jacobian-based method. Section V concludes this paper.

II. TACTILE SERVOING USING CONSTANT TACTILE JACOBIAN

The conventional tactile servoing (see Fig. 1) can be viewed as an optimization problem similar to the visual servoing as follows:

$$\boldsymbol{r}^* = \arg\min_{\boldsymbol{r}} \|\boldsymbol{f}_{\mathrm{c}}(\boldsymbol{r}) - \boldsymbol{f}_{\mathrm{d}}\|, \tag{1}$$

where $\boldsymbol{f}_{\mathrm{c}} \in \mathbb{R}^k$ is the current tactile feature extracted from the current pressure distribution at the current robot end-effector pose $\boldsymbol{r} \in \mathbb{R}^m$. $\boldsymbol{f}_{\mathrm{d}} \in \mathbb{R}^k$ is the desired tactile feature extracted from the desired pressure distribution at the robot end-effector pose $\boldsymbol{r}_{\mathrm{d}} \in \mathbb{R}^m$. $\boldsymbol{f}_{\mathrm{c}}$ is assumed to be a function of $\boldsymbol{r}$ and can be written as $\boldsymbol{f}_{\mathrm{c}}(\boldsymbol{r})$.

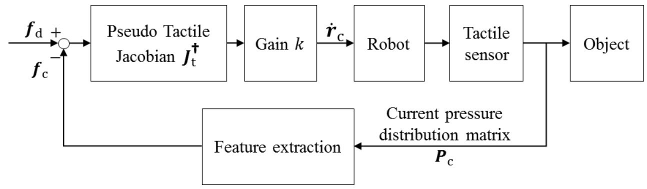

FIGURE 1. Block diagram of the tactile servoing using tactile Jacobian [7]. For the current pressure distribution p_c measured by the tactile sensor, the current tactile feature f_c is extracted. Based on the desired tactile features f_d and the extracted tactile feature f_c, the velocity command to the robot $\dot{r}_c$ is calculated using the tactile Jacobian.

By rewriting (1) using the entire pressure distribution as the tactile feature [14], the optimization problem of the tactile servoing is expressed as

$$\boldsymbol{r}^* = \arg\min_{\boldsymbol{r}} \|\boldsymbol{p}_{\mathrm{c}}(\boldsymbol{r}) - \boldsymbol{p}_{\mathrm{d}}\|, \tag{2}$$

where $\boldsymbol{p}_{\mathrm{c}}(\boldsymbol{r}) \in \mathbb{R}^n$ is the vector of the current pressure distribution at pose $\boldsymbol{r}$, and $\boldsymbol{p}_{\mathrm{d}} \in \mathbb{R}^n$ is a vector of the desired pressure distribution. n is the number of cells of the tactile sensor array. The control law using the tactile Jacobian proposed in [14] is given as follows:

$$\dot{\boldsymbol{r}}_{\mathrm{c}} = -k\boldsymbol{J}^{\dagger}\boldsymbol{e}, \tag{3}$$

where $\dot{\boldsymbol{r}}_{\mathrm{c}} \in \mathbb{R}^m$ is the velocity of the end-effector, k is the gain, $\boldsymbol{J}^{\dagger} \in \mathbb{R}^{m\times n}$ is the pseudo inverse matrix of the tactile Jacobian, and $\boldsymbol{e} = \boldsymbol{p}_{\mathrm{c}}(\boldsymbol{r}) - \boldsymbol{p}_{\mathrm{d}}$ is the deviation between the current and desired pressure distributions. $\boldsymbol{J}^{\dagger}$ relates the pressure distribution deviation to the robot end-effector velocity. By using the least squares method, $\boldsymbol{J}^{\dagger}$ is calculated as follows [14]:

$$\boldsymbol{J}^{\dagger} = \Delta\boldsymbol{R}^{\dagger}\Delta\boldsymbol{P}, \tag{4}$$

where $\Delta\boldsymbol{P} = [\Delta\boldsymbol{p}_{(1)} \;\; \Delta\boldsymbol{p}_{(2)} \;\; \cdots \;\; \Delta\boldsymbol{p}_{(N)}]^{\top}$, and $\Delta\boldsymbol{R} = [\Delta\boldsymbol{r}_{(1)} \;\; \Delta\boldsymbol{r}_{(2)} \;\; \cdots \;\; \Delta\boldsymbol{r}_{(N)}]^{\top}$. $\Delta\boldsymbol{p}_{(i)}$ represents the i-th deviation between desired pressure distribution and the current one. $\Delta\boldsymbol{r}_{(i)}$ represents the corresponding difference of the end-effector poses. N is the total number of data used for the least squares method.

III. TACTILE SERVOING USING A CONVOLUTIONAL NEURAL NETWORK

A. CONVOLUTIONAL NEURAL NETWORK: LeNet-5

The constant tactile Jacobian-based method works well in the vicinity of the desired pressure distribution since the constant tactile Jacobian approximates the relationship between a small deviation of pressure distribution and the corresponding small deviation of the end-effector pose around the desired pressure distribution. The constant tactile Jacobian-based method can control the end-effector around the desired pressure distribution, but does not work for any other given desired pressure distribution.

To solve this problem, we propose a novel tactile servoing scheme using LeNet-5 [16], [17] with appropriate input and output dimensions as shown in Fig. 2. The LeNet-5 used in the proposed control scheme is shown in Fig. 3. The LeNet-5

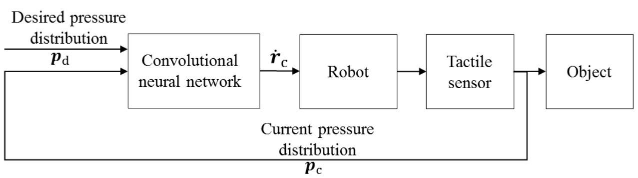

FIGURE 2. **Block diagram of the proposed tactile servoing scheme. The CNN is used to represent the nonlinear relationship between current and desired pressure distributions and the end-effector velocity instead of the tactile Jacobian proposed in our previous method.**

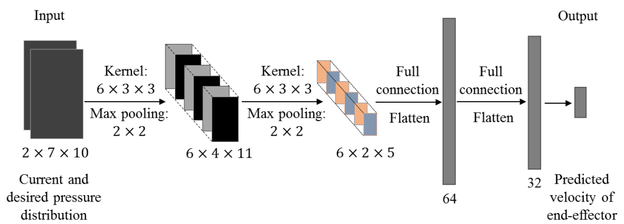

FIGURE 3. **Structure of LeNet-5 used in the proposed tactile servoing scheme. The input includes two pressure distributions, the current and desired ones. Each convolution kernel adopts six filters. In each pooling, max-pooling is used with size 2 × 2 using stride 2. For full connection, two fully connected layers are adopted with 64 neurons and 32 neurons, respectively. The structure of LeNet-5 finally outputs the predicted velocity of the end-effector.**

uses convolution and pooling to extract features. The feature extraction is implemented twice as shown in Fig. 3. The extracted tactile features are converted to the velocity command of the end-effector in the fully connected layers.

The proposed control scheme directly calculates the velocity command of the end-effector from the current and desired pressure distributions at each sampling time. The input and output relation of the proposed control scheme using LeNet-5 is expressed as follows:

$$\dot{\boldsymbol{r}}_c = \boldsymbol{c}(\boldsymbol{p}_c(\boldsymbol{r}), \boldsymbol{p}_d). \tag{5}$$

The proposed scheme works around any desired distributions, because the network is trained for different desired pressure distributions. How to collect the training data set will be discussed later in this section.

B. LOSS FUNCTION

The loss function is defined for evaluating how well the neural network works to train the neural network. The neural network used in the proposed control scheme predicts the desired velocity of the end-effector. This belongs to a regression problem, unlike the pattern recognition problem. The use of mean squared error (MSE) as the loss function is a common approach for regression problems in neural networks. MSE is used as the loss function in the training process of LeNet-5 in the proposed control scheme as well. The loss function is the sum of squared errors between the predicted and ground truth of the desired velocities of the end-effector, which is represented by

$$L = \sum_{i=1}^{N} |\dot{\boldsymbol{r}}_{(i)} - \hat{\dot{\boldsymbol{r}}}_{(i)}|_2, \tag{6}$$

where $\dot{\boldsymbol{r}}_{(i)}$ and $\hat{\dot{\boldsymbol{r}}}_{(i)}$ are the i-th data of the desired and predicted velocities, respectively.

C. TRAINING DATA SET

How to collect the training data set is considered in this subsection. Figure 4 shows the experimental system. The end-effector of the manipulator is equipped with a tactile sensor array, and the tactile sensor array has physical contact with the target object.

The target object consists of nine shafts with roller bearings as shown in Fig. 4. The roller bearings in the shafts of the object are the physical contact points with the robot end-effector. The manipulator has 3 DOF, and the end-effector of the manipulator moves along the y and z-axis, and rotates around the x-axis by a Cartesian control scheme. It can move its end-effector while keeping its physical contact with the object.

The resistive type of tactile sensor array, ShuntMode Matrix Array [18], [19], consists of 70 tactile cells. The dimension of each cell is 8 mm x 5 mm as shown in Fig. 5. Each cell of the array can measure pressure ranging from 0 to 690 [kPa].

The pressure distribution is assumed to be a function of the end-effector pose since the tactile sensor array used in the experimental system is not completely rigid. The training data set is obtained as follows:

1) Randomly select an end-effector pose $\boldsymbol{r}_d = [r_{d,y} \quad r_{d,z} \quad \theta_{d,x}]^\top$ having contact with the object and record its pressure distribution $\boldsymbol{p}_d = [p_{d,1} \quad p_{d,2} \quad \cdots \quad p_{d,70}]^\top$ and the end-effector pose $\boldsymbol{r}_d$ as a desired pressure distribution, and its corresponding end-effector pose.
2) Move the end-effector to a randomly selected pose $\boldsymbol{r}$ around the end-effector pose $\boldsymbol{r}_d$ within ±15 mm in translation and ± 2 degrees in rotation from the end-effector pose $\boldsymbol{r}_d$. Record the pressure distribution and the corresponding pose as $\boldsymbol{p}(\boldsymbol{r})$ and $\boldsymbol{r}$, respectively. Note that the sensor array could cover the object surface within ±15 mm in translation and could be rotated ±2 degrees keeping the contact with the object surface.
3) Move the end-effector from $\boldsymbol{r}$ to $\boldsymbol{r}_d$ linearly and record the velocity of the end-effector $\dot{\boldsymbol{r}}_{(i)}$ and pressure distributions $\boldsymbol{p}(\boldsymbol{r}_{(i)})$ at each sampling time.

We performed a total of 1, 132 processes to collect the training data set. For each process, initial and desired pressure distributions were selected randomly, and the end-effector was moved from $\boldsymbol{r}$ to $\boldsymbol{r}_d$ for five seconds. During each process, 200 data sets were collected and as a result, 226, 400 data sets were obtained. Each data set contains one current and one desired pressure distribution, and the desired velocity of the end-effector. Randomly selected 2, 000 data sets were used as the validation data set, 4, 400 data sets were utilized for the test data set, and 220, 000 data sets were used as the training data set.

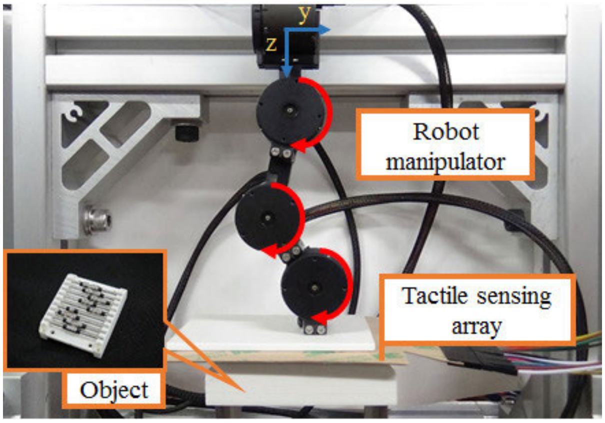

FIGURE 4. Experimental system using 3 DOF manipulator.

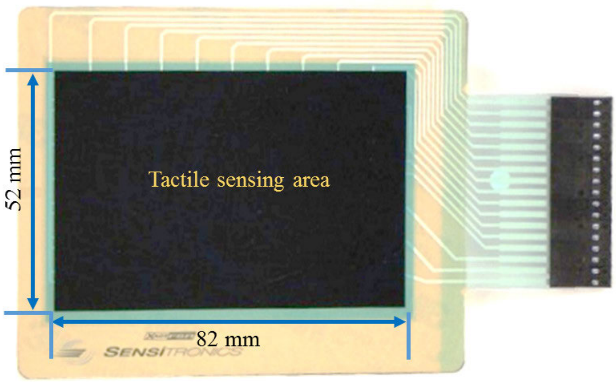

FIGURE 5. ShuntMode Matrix array.

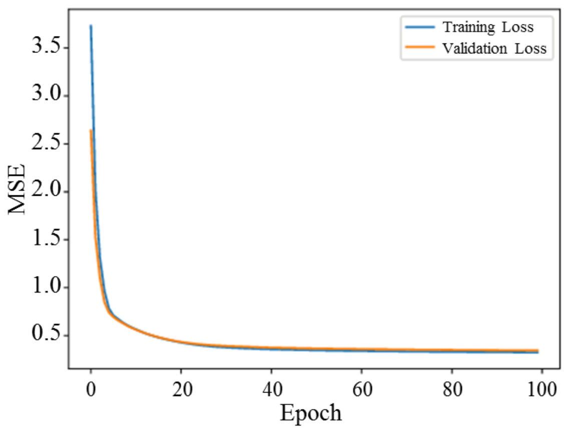

FIGURE 6. Results of the loss function in training process.

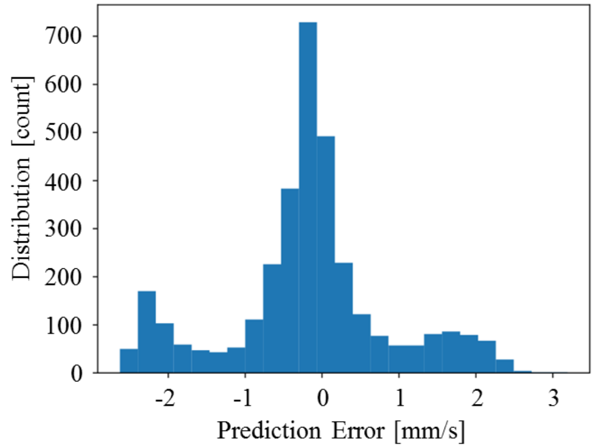

(a) Prediction error of movement along y-axis

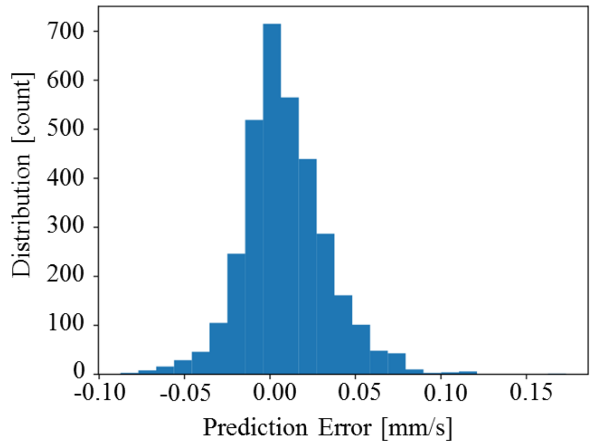

(b) Prediction error of movement along z-axis

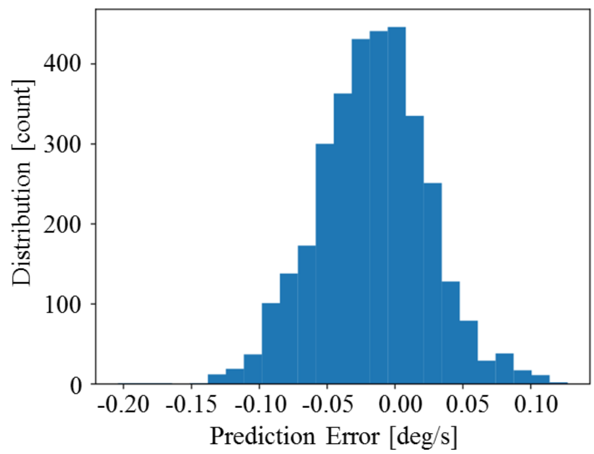

(c) Prediction error of rotation around x-axis

FIGURE 7. Probability distributions in histogram plot of the error in predicted velocities for LeNet-5 used in the tactile servoing scheme.

D. TRAINING RESULTS

Adam optimization and MSE loss functions were used for training the LeNet-5. For validation of the training, 2,000 validation data sets were utilized as mentioned above. The training and validation losses of the training process are shown by blue and yellow lines in Fig. 6, respectively. The training was carried out successfully.

The distributions of the errors between the predicted and the desired velocities using the test data are shown in Fig. 7. While Fig. 7a shows the velocity error distribution along the *y*-axis, Fig. 7b shows that along the *z*-axis, and Fig. 7c shows the angular velocity error distribution around the *x*-axis. The LeNet-5 was trained with reasonable accuracy for the tactile servoing approach we propose in this paper.

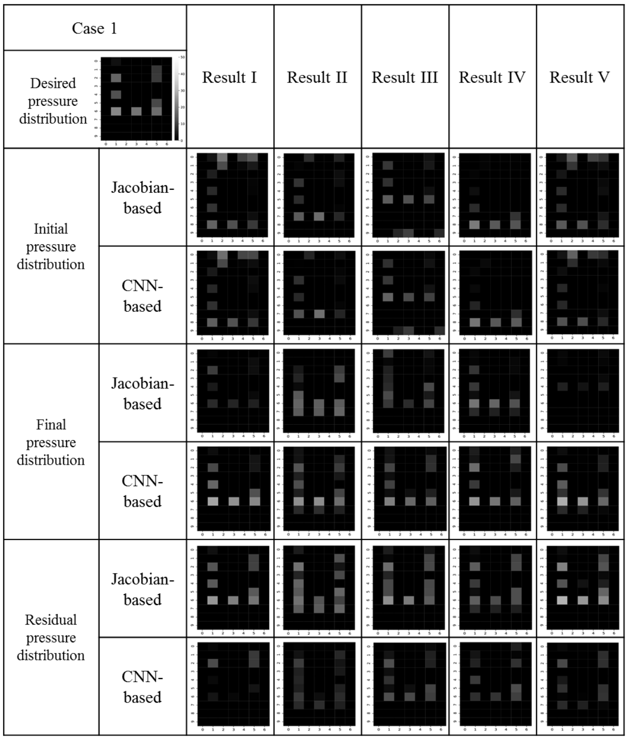

FIGURE 8. Experimental results of Case 1.

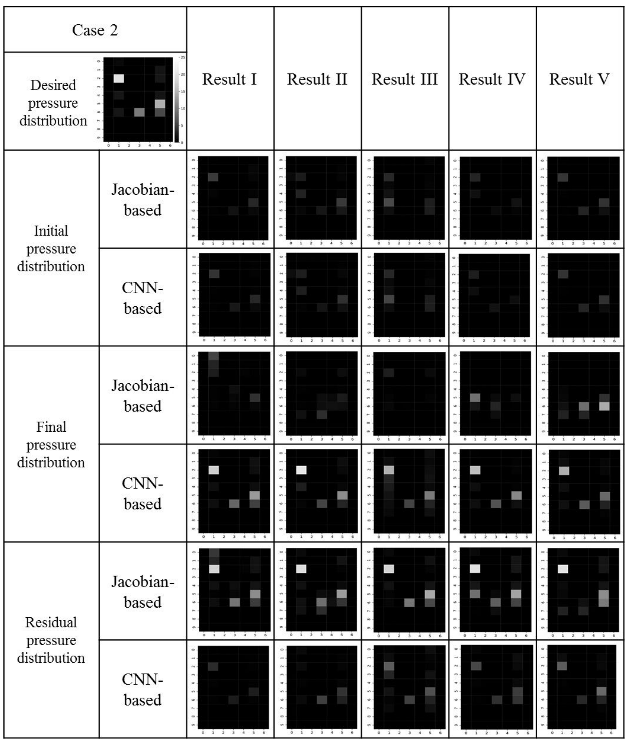

FIGURE 9. Experimental results of Case 2.

IV. EXPERIMENTAL RESULTS

A. CRITERIA FOR EVALUATION OF PROPOSED TACTILE SERVOING CONTROL SCHEME

We use two criteria for evaluating the experimental results, as described below:

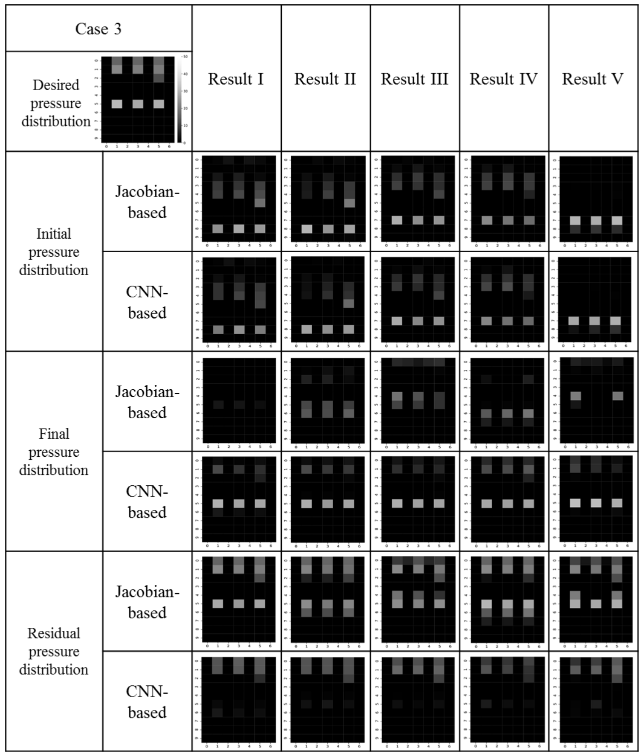

FIGURE 10. Experimental results of Case 3.

- Similarity between the desired pressure distributions and the converged pressure distribution
- Error between the desired pressure distribution and the converged pressure distribution

The similarity between both pressure distributions is computed by a normalized cross-correlation (NCC) defined by

$$P_{\mathrm{ncc}} = \frac{\sum_{i=1}^{n} p_i p_{\mathrm{d},i}}{\sqrt{\sum_{i=1}^{n}(p_i)^2}\sqrt{\sum_{i=1}^{n}(p_{\mathrm{d},i})^2}}, \tag{7}$$

where p_i and $p_{\mathrm{d},i}$ represent the measured and desired values in the i-th tactile cell, respectively. n is the number of tactile cells comprising the tactile sensor. When the current pressure distribution converges to the desired one exactly, P_{ncc} converges to 1. Thus, the high P_{ncc} represents a high similarity between the converged and desired pressure distributions.

In order to evaluate the error between the converged and desired pressure distributions, we utilize root-mean-square error (RMSE), which is the sum of the error between the measured and desired values in each tactile cell. RMSE, P_{rmse}, is computed by:

$$P_{\mathrm{rmse}} = \sqrt{\frac{1}{n}\sum_{i=1}^{n}(p_i - p_{\mathrm{d},i})^2}. \tag{8}$$

B. EXPERIMENTS

We experimentally compare the performance of the proposed control scheme with that of the constant tactile Jacobian-based scheme. The experiments are conducted for

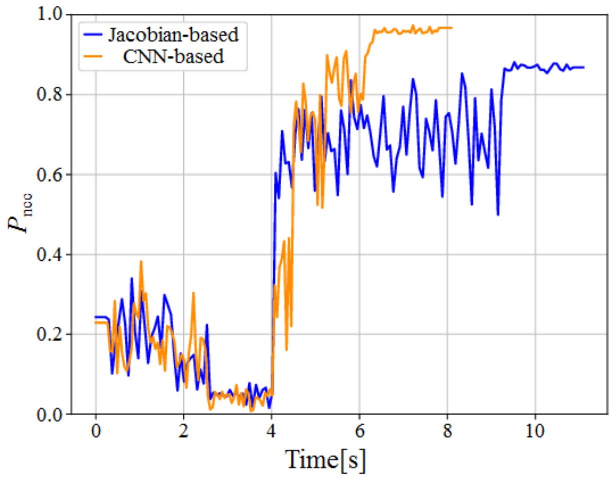

(a) Evaluation by P_{ncc}

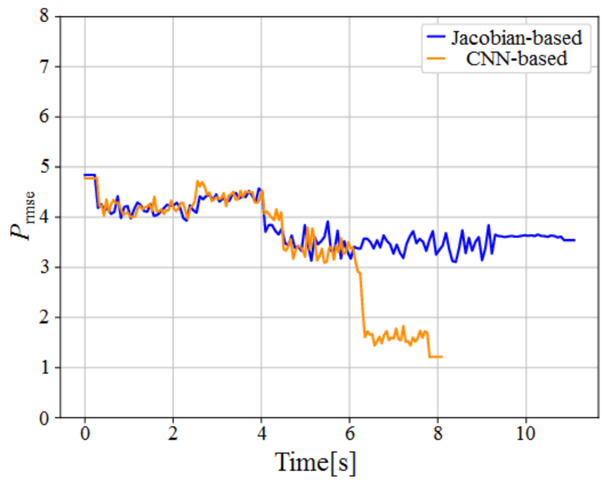

(b) Evaluation by P_{rmse}

FIGURE 11. Evaluation for pressure distribution in tactile servoing scheme.

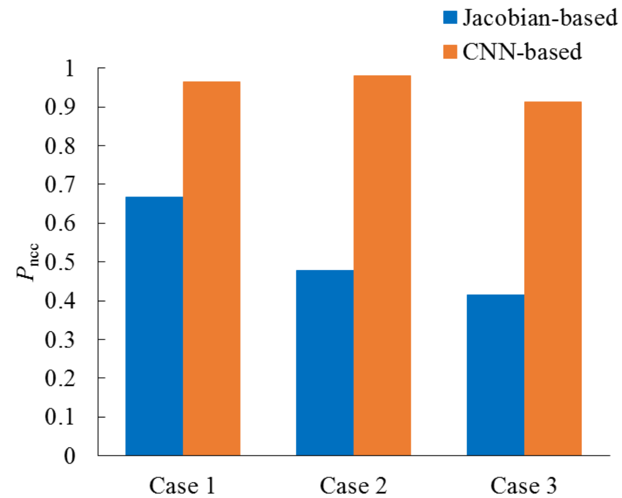

FIGURE 12. Average P_{ncc} of the constant tactile Jacobian-based and proposed method.

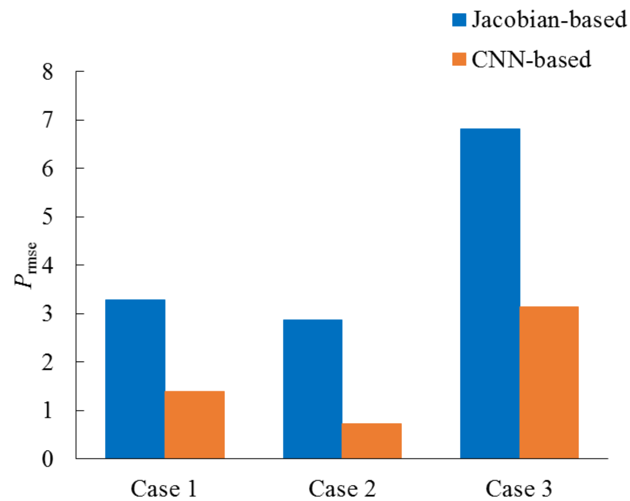

FIGURE 13. Average P_{rmse} of the constant tactile Jacobian-based and proposed method.

three different desired pressure distributions using both the constant tactile Jacobian-based scheme and the proposed tactile servoing scheme. For each desired pressure distribution using each scheme, the experiments are performed five times. The initial pressure distribution of each trial was selected as much as identical. Fig. 8, Fig. 9, and Fig. 10 show the experimental results.

Figure 8 contains the experimental results of the desired pressure distribution, Case 1. The desired pressure distribution is selected corresponding to a pose in the vicinity of the area where the training data sets were collected. For the presentation of the experimental results, initial pressure distributions, final pressure distributions, and residual pressure distributions are shown. The residual pressure distribution shows the deviation of the final pressure distribution from the desired pressure distribution. Figure 11 shows an example of the transient response of P_{ncc} and P_{rmse} for Result 1 of Case 1 shown in Fig. 8. When P_{ncc} is kept equal to or larger than 0.9 over 1.5 second, the pressure distribution is considered to have converged to the desired pressure distribution. Figure 8 shows that the residual pressure distribution of the proposed CNN-based scheme is much smaller than that of the constant tactile Jacobian-based scheme.

Figure 9 shows the experimental results for the desired pressure distribution, Case 2. The desired distribution of Case 2 is also selected corresponding to a pose in the vicinity of the area where the training data sets were collected, but the total force along z direction is about two times of the Case 1. The sum of the pressures of each cell for Case 1 is 97 [kPa], while the sum of the pressures for Case is 142 [kPa]. Similar to Case 1, the residual pressure distribution of the proposed CNN-based scheme is much smaller than that of the constant tactile Jacobian-based scheme.

Figure 10 shows the experimental results for the desired pressure distribution, Case 3. The desired pressure distribution of Case 3 is selected outside of the area where the training data sets were collected. Similar to the cases, the residual pressure distribution of the proposed CNN-based scheme is much smaller than that of the constant tactile Jacobian-based scheme.

Fig. 12 and Fig. 13 show the average of P_{ncc} and the average of P_{rmse} for the cases, respectively. The proposed scheme has higher NCC and smaller RMSE for all of the cases.

According to the validation experimental results, we confirm that the proposed scheme can achieve more precise physical contact compared to the constant tactile Jacobian-based scheme.

V. CONCLUSION

In this paper, we propose a novel pressure distribution-based tactile servoing control scheme of a manipulator that has physical interaction with the environment. The proposed method utilizes a convolutional neural network, LeNet-5, to represent highly nonlinear relationships among the robot velocity command, current pressure, and desired pressure distributions. The proposed method enabled a robot to touch its surroundings more precisely than with the conventional method, and also the experimental results show that the proposed method has better performance than that of the constant tactile Jacobian-based method. In this paper, the pressure distribution is assumed to be a function of the end-effector pose. The system could be used for several applications including the physical human-robot interaction. We believe that our method can facilitate the advancement of solutions for the issues in tactile robot-human interaction.

REFERENCES

[1] T. Mukai, S. Hirano, H. Nakashima, Y. Kato, Y. Sakaida, S. Guo, and S. Hosoe, "Development of a nursing-care assistant robot RIBA that can lift a human in its arms," in *Proc. IEEE/RSJ Int. Conf. Intell. Robots Syst.*, Oct. 2010, pp. 5996–6001.

[2] M. Khoramshahi, G. Henriks, A. Naef, S. S. M. Salehian, J. Kim, and A. Billard, "Arm-hand motion-force coordination for physical interactions with non-flat surfaces using dynamical systems: Toward compliant robotic massage," in *Proc. IEEE Int. Conf. Robot. Autom. (ICRA)*, May 2020, pp. 4724–4730.

[3] R. C. Luo, C. P. Tsai, and K. C. Hsieh, "Robot assisted tapping control for therapeutical percussive massage applications," in *Proc. IEEE Int. Conf. Robot. Autom. (ICRA)*, May 2017, pp. 3606–3611.

[4] C. Wang and J. P. Whitney, "Series elastic force control for soft robotic fluid actuators," 2020, *arXiv:2004.01269*. [Online]. Available: http://arxiv.org/abs/2004.01269

[5] A. D. Berger and P. K. Khosla, "Using tactile data for real-time feedback," *Int. J. Robot. Res.*, vol. 10, no. 2, pp. 88–102, Apr. 1991.

[6] L. Weiss, A. Sanderson, and C. Neuman, "Dynamic sensor-based control of robots with visual feedback," *IEEE J. Robot. Autom.*, vol. RA-3, no. 5, pp. 404–417, Oct. 1987.

[7] P. Sikka, H. Zhang, and S. Sutphen, "Tactile servo: Control of touch-driven robot motion," in *Experimental Robotics III*. Berlin, Germany: Springer, 1994, pp. 219–233.

[8] N. N. Chen, H. Zhang, and R. E. Rink, "Touch-driven robot control using a tactile Jacobian," in *Proc. Int. Conf. Robot. Autom.*, 1997, pp. 1737–1742.

[9] N. Chen, H. Zhang, and R. Rink, "Tactile sensing of point contact," in *Proc. IEEE Int. Conf. Syst., Man Cybern. Intell. Syst. 21st Century*, 1995, pp. 574–579.

[10] N. Chen, H. Zhang, and R. Rink, "Edge tracking using tactile servo," in *Proc. IEEE/RSJ Int. Conf. Intell. Robots Syst. Human Robot Interact. Cooperat. Robots*, 1995, pp. 84–89.

[11] H. Zhang and N. N. Chen, "Control of contact via tactile sensing," *IEEE Trans. Robot. Autom.*, vol. 16, no. 5, pp. 482–495, Oct. 2000.

[12] Q. Li, C. Schurmann, R. Haschke, and H. Ritter, "A control framework for tactile servoing," in *Proc. Int. Conf. Robot., Sci. Syst. IX (RSS)*, 2013, doi: 10.15607/RSS.2013.IX.045.

[13] Z. Kappassov, J.-A. Corrales, and V. Perdereau, "Touch driven controller and tactile features for physical interactions," *Robot. Auto. Syst.*, vol. 123, Jan. 2020, Art. no. 103332.

[14] C. T. Wen, J. Kinugawa, S. Arai, and K. Kosuge, "Tactile servo based on pressure distribution," in *Proc. IEEE Int. Conf. Mechatronics Autom. (ICMA)*, Aug. 2019, pp. 868–873.

[15] M. Lopez and W. Yu, "Nonlinear system modeling using convolutional neural networks," in *Proc. 14th Int. Conf. Electr. Eng., Comput. Sci. Autom. Control (CCE)*, Oct. 2017, pp. 1–5.

[16] Y. LeCun, L. Bottou, Y. Bengio, and P. Haffner, "Gradient-based learning applied to document recognition," *Proc. IEEE*, vol. 86, no. 11, pp. 2278–2324, Nov. 1998.

[17] A. Krizhevsky, I. Sutskever, and G. E. Hinton, "ImageNet classification with deep convolutional neural networks," *Commun. ACM*, vol. 60, no. 2, pp. 84–90, Jun. 2012.

[18] *Sensitronics LCC*. Accessed: Oct. 10, 2020. [Online]. Available: https://www.sensitronics.com/products-shunt-mode-matrix-array.php

[19] *ShuntMode Matrix Array*. Sensitronics LCC. Accessed: Oct. 10, 2020. [Online]. Available: https://www.fabtolab.com/force-sensitive-resistor-shunt-mode-matrix

CHEN-TING WEN received the B.S. degree in mechanical engineering from National Cheng Kung University, Tainan, Taiwan, in 2012, and the M.S. degree in biorobotic from the School of Engineering, Tohoku University, Sendai, Japan, in 2015, where he is currently pursuing the Ph.D. degree in engineering. His research interests include tactile sensing ability and tactile servo.

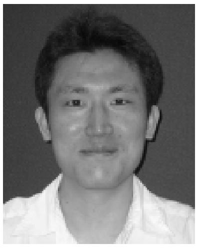

SHOGO ARAI (Member, IEEE) received the B.S. degree in aerospace engineering and the M.S. and Ph.D. degrees in information sciences from Tohoku University, Sendai, Japan, in 2005, 2007, and 2010, respectively.

From 2010 to 2016, he was an Assistant Professor with the Intelligent Control Systems Laboratory, Tohoku University. In 2016, he joined the System Robotics Laboratory, Department of Robotics, Tohoku University, as an Associate Professor, where he is currently an Associate Professor. His research interests include robot vision, machine vision, 3D measurement, production robotics, networked control systems, and multi-agent systems.

Dr. Arai received the Young Scientists' Award from the Commendation for Science and Technology by the Minister of Education, Culture, Sports, Science and Technology, in 2021; the Best Paper Award from FA Foundation, in 2019, the 32th Best Paper Award from the Robotics Society of Japan, in 2019, the Certificate of Merit for the Best Presentation from The Japan Society of Mechanical Engineers, in 2019, the Best Paper Award Finalist at the IEEE International Conference on Mechatronics and Automation, in 2012, and the Excellent Paper Award from The Institute of Systems, Control and Information Engineers, in 2010.

JUN KINUGAWA (Member, IEEE) received the Ph.D. degree in bio-engineering and robotics from Tohoku University, Sendai, Japan, in 2011. From 2011 to 2021, he was an Assistant Professor with the Department of Robotics, Tohoku University. Since 2021, he has been with the Faculty of Symbiotic Systems Science, Fukushima University, as an Associate Professor. His research interests include human–robot interaction, co-worker robot, robotic hand, and power assistive systems. He is a member of the IEEE Robotics and Automation Society (IEEE RAS).

KAZUHIRO KOSUGE received the B.S., M.S., and Ph.D. degrees in control engineering from Tokyo Institute of Technology, in 1978, 1980, and 1988, respectively. After having served as a Research and Development Staff for the Production Engineering Department, Nippon Denso Company Ltd., a Research Associate for Tokyo Institute of Technology, and an Associate Professor for Nagoya University, he joined Tohoku University, as a Professor, in 1995, and served as a Distinguished Professor, from 2018 to March 2021. He joined the Department of Electrical and Electronic Engineering, The University of Hong Kong, as the Chair Professor, in June 2021. He is currently the Director of the Center for Transformative AI and Robotics and a Specially Appointed Professor of the Graduate School of Engineering, Tohoku University, Japan. He is a JSME Fellow, a SICE Fellow, a RSJ Fellow, and a JSAE Fellow, and a member of the Engineering Academy of Japan. He received the Medal of Honor and the Medal with Purple Ribbon from the Government of Japan—a national honor in recognition of his prominent contributions to academic and industrial advancements, in 2018. He also received IEEE RAS George Saridis Leadership Award in robotics and automation, in 2021, for his exceptional vision of innovative research and outstanding leadership in the robotics and automation community through technical activity management. He was the President of the IEEE Robotics and Automation Society, from 2010 to 2011; the IEEE Division X Director, from 2015 to 2016; and the IEEE Vice President for Technical Activities, in 2020.